Statistical Mechanics of Prion Diseases

A. Slepoy, R. R. P. Singh, F. Pázmándi, R. V. Kulkarni, and D. L. Cox
Department of Physics, University of California, Davis, California 95616
(Received 27 February 2001; published 12 July 2001)

We present a two-dimensional, lattice based, protein-level statistical mechanical model for prion diseases (e.g., mad cow disease) with concomitant prion protein misfolding and aggregation. Our studies lead us to the hypothesis that the observed broad incubation time distribution in epidemiological data reflect fluctuation dominated growth seeded by a few nanometer scale aggregates, while much narrower incubation time distributions for innoculated lab animals arise from statistical self-averaging. We model "species barriers" to prion infection and assess a related treatment protocol.

DOI: 10.1103/PhysRevLett.87.058101 PACS numbers: 87.19.Xx, 05.20.Dd, 87.15.He

Transmissible neurodegenerative prion diseases, such as mad-cow disease (BSE) and Creutzfeldt-Jakob disease (CJD) in humans, increasingly represent a serious public health threat [1]. Prusiner and collaborators have shown that the infectious agent (prion) in these diseases consists of a quantity of a misfolded form (PrP^{Sc}) of the $\sim$200 amino acid PrP^{C} protein which is expressed ubiquitously in mammalian neurons [2]. The PrP^{C} proteins normally reside on neuron surfaces [3], and the more hydrophobic PrP^{Sc} forms tend to aggregate: large (micron scale) PrP^{Sc} amyloid plaques are a common postmortem feature of brain tissues [1]. Nucleic acid free propagation demands that PrP^{Sc} autocatalyze their own formation by helping to convert more PrP^{C} into PrP^{Sc} [2,4]. Given that mammalian PrP^{c} differ by only 5%–10% in amino acid composition and that variant CJD correlated with BSE has been observed, the efficacy of "species barriers" in limiting transmission is of considerable interest.

Several facts suggest that the incubation of prion diseases may be driven less by complex biology (as in Alzheimers' disease) than by physico-chemical processes, including (1) the "universal character" of sporadic CJD, observed globally without evident spatiotemporal clustering at an annual background death rate of 0.5–1.5 per 10^6 and mean onset age of about 63 years [5]. (2) The long incubation period is followed by rapid neurodegeneration and death. (3) Reproducible mean incubation time vs infectious dose relations are observed in laboratory animal studies [6]. (4) PrP^{Sc} may be grown *in vitro* without biological processing and is toxic to neurons, though not yet demonstrably infectious [7]. The following question is thus raised: *Is the incubation time of prion disease dominated by a fundamental physico-chemical nucleation and growth of PrP^{Sc} aggregates?*

We present a two-dimensional, statistical mechanical model for prion disease based at the protein level. It is all but hopeless to develop an atomic level simulation capable of spanning the 21 temporal orders of magnitude between picosecond scale intraprotein motion and the potentially decades long incubation times of prion aggregates. Our simulation is a bridge between the short distance and time scales covered in individual protein models and the long time, macroscopic realm of chemical kinetics. We use our simulations to identify the protectorate of principles necessary to describe the aforementioned universal features of prion disease. Specifically, we find (1) concomitant PrP^{Sc} autocatalysis and stable aggregation can explain the long disease incubation times, and the difference between sporadic (unseeded) and infectious (seeded) onset. This principle is consistent with data for yeast prions [8], is closely related to the earlier nucleation theory of Come *et al.* [9], and avoids the need to fine-tune model parameters with separated autocatalysis and aggregation [10]. (2) The distributions of disease incubation times (broad fluctuation driven spectrum for dilute prion doses, narrow short time shifted distribution for more concentrated prion doses) strongly suggest a central role for growth from a minimally nanometer scale seed (with order 10 PrP^{Sc} proteins). With these assumptions we obtain a one parameter fit to the inferred BSE incubation time distribution, an order of magnitude correct estimate of the mean incubation time for BSE and infectious CJD, and we argue that self-averaging explains a narrowing of incubation time distributions observed in the laboratory [6,11]. Finally, we generalize our model to describe the species barrier and provide theoretical underpinning to proposed treatments based upon coating of incipient prion plaques.

Our model is motivated by several epidemiological and experimental facts. (i) There is an order of magnitude separation between mean incubation times for infectious and sporadic forms of the disease. (ii) For infectious diseases, the onset times are much longer than the late-stage doubling time [12]. (iii) There is no experimental evidence for stable PrP^{Sc} monomers *in vivo* or *in vitro* without exceptional pH and ligation conditions [13]. (iv) Studies of yeast prions support a conflation of autocatalysis and aggregation [8], in contrast to the usually assumed separation in the standard prion picture [2,9]. (v) One-dimensional fibril aggregation arises for the stable PrP^{C} cores obtained after protease attack, while whole prion proteins tend towards amorphous aggregates [14]. (vi) PrP^{C} is a neuron surface based glycoprotein.

Our fundamental hypothesis is that the incubation time is dominated by aggregation from an individual seed on the surface of a single neuron. Thus, we develop a molecular automata model focusing on this phenomenon. Adopting Occam's philosophy of seeking an adequate description with a minimal number of assumptions and parameters, we have surveyed a broad spectrum of automata rules, which will be reported in detail elsewhere. To motivate the rules for the present simulations, it is important to note two general strategies that fail to fully describe the prion phenomena. These are (i) rules that allow for stable misfolded monomers and dimers. These lead to heterogeneous runaway growth and are inconsistent with low incidence of sporadic diseases [10]. (ii) One-dimensional fibril aggregation. The incubation time distribution in this case can be fit well to the gamma distribution, which agrees with BSE data [15], but yields late-stage doubling times comparable to single seed incubation times, and incubation time distributions which are too narrow to fit the BSE data [15]. The essential reason for this is the zero-dimensional fibril surface, which fixes attachment rates to be size independent.

Our minimal model, which seems adequate to describe the above phenomena, consists of cellular automata in which monomers diffuse on a hexagonal lattice (which minimizes anisotropy effects). The lattice structure matters little for long-time phenomena, which is also confirmed by fits of simulation data to lattice independent analytic distributions (discussed later).

The simulation rules characterizing the prion "protectorate" are as follows (displayed schematically in Fig. 1): First, individual lattice cells take on three values: unoccupied (implicitly filled with water), occupied by a PrP^C protein, or occupied by a PrP^{Sc} protein. At the beginning of each simulation, we choose a monomer PrP^C configuration distributed randomly, with or without a PrP^{Sc} seed, located randomly as well. We perform site-by-site sweeps of our lattice (one sweep sets our time scale), updating according to the following rules (d is the nearest neighbor coordination for a given monomer):

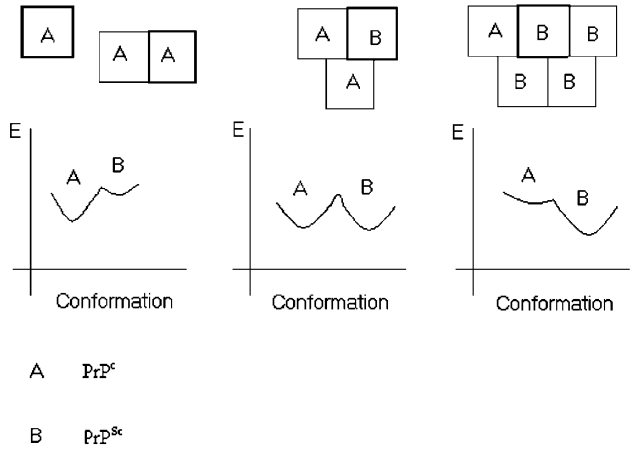

FIG. 1. Simulation rules and energy landscapes for model prion proteins. Upper figures show proteins in varying coordination environments corresponding to rules (1)–(6); lower figures show schematic energy landscapes [16], for highlighted monomers consistent with rules and observations.

(1) Identify each occupied cell as PrP^C or PrP^{Sc} by checking its number of nearest neighbors. (2) For each PrP^C, move one step in a random direction if that adjoining site is unoccupied. (3) Identify aggregates (size N_P) by PrP^{Sc} presence; move them per rule (2) with probability $1/\sqrt{N_p}$. (4) For $d = 0, 1$ the protein remains PrP^C. (5) For $d = 2$, the protein is PrP^C or PrP^{Sc} with equal probability. (6) For $d \geq 3$ the protein is PrP^{Sc}.

We also maintain a constant average PrP^C concentration, randomly siting a new PrP^C for each one lost in the previous sweep, though our results do not strongly depend upon this condition.

Rules (1)–(3) ensure diffusive motion of PrP^C monomers and PrP^{Sc} aggregates. Rules (4)–(6) specify protein interactions and autocatalysis and reflect the fact that sequestering the proteins from water can cause a restructuring of hydrophobic parts thus changing the overall structure. These rules ensure the absence of stable misfolded monomers and dimers, thus making it difficult to nucleate new seeds [16,17]. This separates the time scales for sporadic and infectious diseases. They also imply that stable aggregation needs a simultaneous assembly of two or more monomers, thus mimicking oligomerization as an intermediate step to aggregation [8].

We then sample the distribution of times required to reach a given aggregate size $\mathcal{A}$ from our seeds (the hypothesized incubation time distribution). This procedure is repeated for up to millions of full sweeps through the lattice. A sweep defines the minimum time scale for conversion of PrP^C to PrP^{Sc}, which is presumably of order a second or less in real time. We work with maximum lattice sizes of $N = 4 \times 10^4$. Practically, we are able to run at areal monomer concentrations $c \geq 0.1\%$, which are likely to be about 3 orders of magnitude larger than in the brain.

The distribution of incubation times starting from an initial seed of 10 PrP^{Sc} monomers [18] and growing up to a final aggregate size of $\mathcal{A} = 0.2\%\ N$ (80 monomers) for various monomer concentrations, c, is displayed in Fig. 2a. There is greater fluctuation for small c, and increasing c shifts P_1 to short times. The distribution shape is independent of concentration [Fig. 2(b)] when t is scaled by the mean time t_m; we find that t_m is well described either by a scaling law $t_m(c) \propto c^{-\alpha(\mathcal{A})}$ with $\alpha(\mathcal{A}) \leq 2$, or by a sum of monomer and dimer terms $t_m(c) = A/c^2 + B/c$. The latter result is consistent with an approximate analytic theory in which we assume shell-by-shell growth dominated by the attachment of dimers with "filling in" by monomers. This theory has a basic dimer attachment probability per sweep of $p(n) = p_0 + p_1 n$, where n is the number of attached dimers up to that time and grows with the radius of the aggregate. This "shell model," which we believe is new in the nucleation-aggregation literature, implies that aggregation accelerates with size, with exponential runaway of mean aggregate size at long times in contrast to

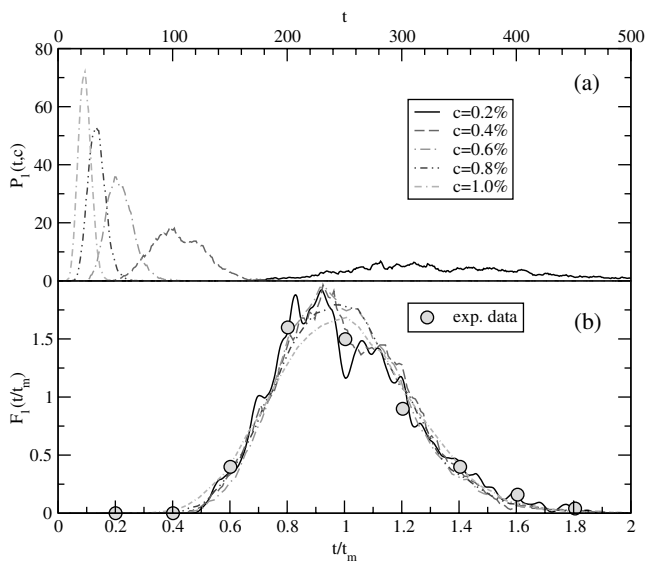

FIG. 2. Aggregation lifetime distributions $P_1(t, c)$ from a seed with ten proteins, simulations terminate at aggregate size $\mathcal{A} = 80$, and time is measured in units of 10^4 full lattice sweeps. (a) Dependence upon areal concentration c of normal prion proteins. (b) Scaled distribution $F_1(t/t_m)$ vs t/t_m. t_m is the mean lifetime for a given concentration. Points are the inferred incubation time distribution for BSE-infected cattle in the United Kingdom born in 1987 [15].

the typical power law growth. The resulting aggregation time distribution is of the beta form in $x = \exp(-p_1 t)$ with $P_1(\mathcal{A}, t) \propto x^{p_0/p_1}(1 - x)^{\tilde{\mathcal{A}}}$, where $\tilde{\mathcal{A}}$, the number of dimer attachments, depends on $\mathcal{A}$. This approximation produces a good fit to our data. This form for P_1 fits our data well.

Taken together, these data and approximate theory provide strong evidence for *asymptotic compression* of P_1: for $c \to 0$, an increasingly large range of $\mathcal{A}$ will have essentially the same scaled shape, because the time t_2 it takes to go from $\mathcal{A}$ to say, $2\mathcal{A}$, will be much smaller than t_m for going from $10 \to \mathcal{A}$. Indeed, in extrapolating our results for $0.2\% \le c \le 1\%$ to biological c values of order 0.001%, we find t_2 to be about $0.1 t_m$ with $\mathcal{A} = 80$.

This has implications for disease propagation: other processes such as protease attack or competition between PrP^{Sc}-PrP^{Sc} and PrP^{Sc}-neuron binding will limit prion aggregation on the neural surface and cause fissioning and spreading of nanoaggregates to other neurons [19]. Such fission leads to rapid late-stage exponential growth, as noted previously [20]. At the order-of-magnitude level t_2 sets the doubling time for disease spread. Given $t_2 \ll \bar{t}$, slow growth fluctuations for small seed aggregates dominate the overall incubation time, ensuring that the broad distributions survive. This is in contrast to the linear fibril aggregates, for which the two time scales are comparable and the need for many doubling periods implies that the distribution will narrow considerably. Such a separation of time scales has been seen in hamster experiments, where the first observable levels of PrP^{Sc} in brain tissues occur at about 90 days, with symptom onset at 120 days, and a doubling time of 2 days [12].

We stress several points of agreement with observation and laboratory data: (1) Our lifetimes are in order of magnitude agreement with observed BSE incubation times and new variant CJD death ages. Extrapolating the peak of our lowest c data to an areal concentration of $c = 10^{-3}\%$ suggested by the literature estimate of 100 nanomole/liter [21], we get an estimated incubation time of about 10^8 sweeps. Assuming a basic misfolding time (single sweep) of about one second which is reasonable at the order of magnitude level, we obtain about five years for BSE or vCJD, which is clearly of the right order. (2) By simply scaling time for $\mathcal{A} = 80$ by the mean time t_m, we achieve an exceptionally good fit of the inferred incubation time distribution for BSE in the United Kingdom (for cattle born in 1987) [15] to our scaling curve as shown in Fig. 2(b). This supports our hypothesis that autocatalytic aggregation seeded by a few prion nanoaggregates triggered the BSE disease. This is very plausible since (i) infection is believed to have come from rendering plant offal derived from many animals after considerable processing, leading to substantial dilution, and (ii) prion transmission by oral consumption is estimated to be less efficient by a factor of 10^9. (3) We obtain results for sporadic (unseeded) disease consistent qualitatively with the 1 in 10^6 occurrence frequency. Our sporadic P_1 curves are different in shape, completely dimer dominated ($t_m \propto c^{-2}$), and for our estimated biological concentration of $10^{-3}\%$, could peak at about 1000 yr. Unfortunately, the short time tail is unresolvable with our current simulation statistics.

The dose dependence of the incubation times in our model is not unique. Unlike the case of fibrils, where it is not sensitive to size of "seeds" and depends logarithmically on the dose concentration, D (see also [20]), in our case the incubation times depend on seed size, and can be either dose independent, or logarithmic, or even a power law [6]. Dosing by a large number of seeds residing on different neurons will induce self-averaging that will narrow the incubation time distribution, moving it towards shorter times, evidently as $1/\sqrt{D}$ for truly independent seeds. Several *in vivo* experiments show distribution time narrowing with increased dosage but are not amenable to quantitative analysis at this time [11].

We turn now to the species barrier. We model it in terms of two parameters: (i) p, which relates to the strength of mutual misfolding catalysis and (ii) q, which relates to physisorption between the species. For a protein of species one, let N be the number of same species neighbors and N' the number of alien neighbors. The protein sees a reduced effective coordination of $x = N + pN'$. The misfolding probability is a sharp function of x and can be taken as $f(x) = [\exp(\beta x) + 1]^{-1}$ with large β. The parameter p (chosen less than unity) provides a measure of the reduced effectiveness of interspecies catalysis. To account for the variation in physisorption,

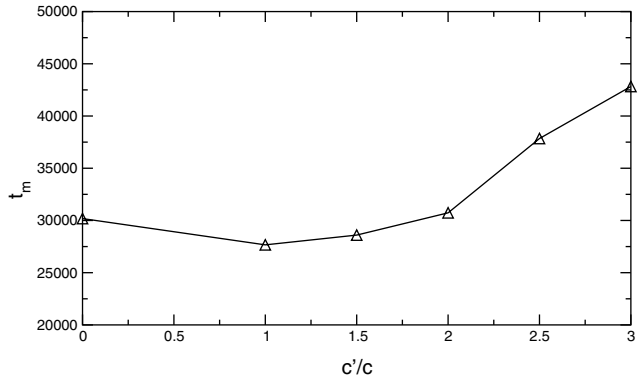

FIG. 3. Mean incubation time t_m vs relative concentration of alien prions c'/c (test of coating treatment; see text for discussion).

we allow a $PrP^{C,Sc}$ cluster of mass M ($M = 1$ being a monomer) to desorb from an alien prion aggregate with probability q^K/M, where K is the number of units in the cluster. For the second species, we similarly define the parameters, p' and q'. Making $p \neq p'$ and $q \neq q'$ allows us to model one of the most striking aspects of the species barrier, namely, its asymmetry (e.g., mice infect hamsters well; hamsters infect mice poorly).

We have used this species barrier generalization to model a potential treatment for prion diseases. Suppose the asymmetry is such that p("mouse") $\ll p'$("hamster"). In this case, $PrP^{Sc'}$ is more favorably formed from $PrP^{C'}$ in the presence of a seed aggregate of PrP^{Sc} than PrP^{Sc} is formed from PrP^{C} in the presence of a $PrP^{Sc'}$ seed. Thus, by injecting a large enough initial dose of alien $PrP^{C'}$ proteins into the organism, it should be possible for $PrP^{C'}$ to compete favorably with PrP^{C} for aggregation and extend the incubation time. Such protocols have been tested experimentally: (i) Experiments with the coating dye molecule Congo red [22] reveal a surprising *nonmonotonic* dose vs lifetime relation: small Congo red concentrations yield a reduced time for incubation, while larger Congo red concentrations significantly extend the incubation time. (ii) *In vitro* experiments show that the above coating scenario with alien prions works [23] when the initial $PrP^{C'}$ concentration $c' > c$.

We find both of these experimental features in our simulation as shown in Fig. 3. For $c'/c < 2$, the incubation time is slightly shortened, while for $c'/c > 2$ the incubation time is increased. We find that the lifetime shortening arises because once a few $PrP^{C'}$ aggregate, they partially block the motion of adjacent PrP^{C} proteins, enhancing the likelihood of host protein misfolding. However, further PrP^{C} misfolding is significantly reduced once $PrP^{Sc'}$ coats the seed.

In conclusion, we have developed a new approach to the calculation of incubation times in amyloid diseases, which bridges the gap between the relatively short time studies of protein folding and long-time kinetic approaches. We have shown that there are several possible "universality classes" of amyloid aggregation. We have constructed a model, which has (i) clear separation of sporadic and infectious time scales, (ii) incubation times dominated by early-stage growth from small seeds followed by rapid late stage growth, and (iii) broad distribution of incubation times consistent with BSE data. (iv) We have also tested a treatment protocol based on the asymmetric species barrier, which shows the further usefulness of such a simple model.

We acknowledge useful discussions with S. Carter, F. Cohen, F. DeArmond, R. Fairclough, C. Ionescu-Zanetti, T. Jue, R. Karana, and C. Lasmézas. R. R. P. S. and D. L. C. have benefited from discussions at workshops of the Institute for Complex Adaptive Matter. We are grateful for a grant of supercomputer time from the Lawrence Livermore National Laboratory. F. P. acknowledges support from U.S. NSF Grant No. NSF DMR-9985978 and Hungarian NSF Grant No. OTKA 29236.

[1] A. Coghlan, New Sci. **168**, 4 (2000).
[2] S. B. Prusiner, in *Prion Biology and Diseases,* edited by S. B. Prusiner (Cold Spring Harbor Laboratory Press, Cold Spring Harbor, NY, 1999), p.1.
[3] S. B. Prusiner *et al.,* in *Prion Biology and Diseases,* Ref. [2], p. 349.
[4] J. S. Griffith, Nature (London) **215**, 1043 (1967).
[5] R. G. Will *et al.,* in *Prion Biology and Diseases,* Ref. [2], p. 465.
[6] S. B. Prusiner *et al.,* in *Prion Biology and Diseases,* Ref. [2], p. 113.
[7] K. Post *et al.,* Arch. Virol. (Suppl.) **16**, 265 (2000).
[8] T. R. Serio *et al.,* Science **289**, 1317 (2000).
[9] J. H. Come, P. E. Fraser, and P. T. Lansbury, Jr., Proc. Natl. Acad. Sci. U.S.A. **90**, 5959 (1993).
[10] M. Eigen, Biophys. Chem. **63**, A1 (1996).
[11] C. I. Lasmézas *et al.,* Science **275**, 402 (1997).
[12] M. Beekes, E. Baldauf, and H. Diringer, J. Gen. Virol. **77**, 1925 (1996).
[13] D. O. V. Alonso *et al.,* Proc. Natl. Acad. Sci. U.S.A. **98**, 2985 (2001).
[14] W. Swietnicki *et al.,* Biochemistry **39**, 424 (2000).
[15] D. J. Stekel, M. A. Nowak, and T. R. E. Southwood, Nature (London) **381**, 119 (1996); R. M. Anderson *et al.,* Nature (London) **382**, 779 (1996).
[16] For a review, see J. N. Onuchic, Z. Luthey-Schluten, and P. G. Wolynes, Annu. Rev. Phys. Chem. **48**, 545 (1997).
[17] For a similar coordination rule, see M. Horiuchi and B. Caughey, Structure Folding Design **7**, R231 (1999).
[18] The minimally stable seven monomer seed exhibits spurious barriers for transition to a ten monomer seed.
[19] M. A. Nowak *et al.,* Integrative Biol. **1**, 3 (1998).
[20] J. Masel, V. A. A. Jansen, and M. A. Nowak, Biophys. Chem. **77**, 139 (1999).
[21] M. Laurent, FEBS Lett. **407**, 1 (1997).
[22] R. Demaimay *et al.,* J. Neurochem. **71**, 2534 (1998); H. Rudyk *et al.,* J. Gen. Virol. **81**, 1155 (2000).
[23] M. Horiuchi *et al.,* Proc. Natl. Acad. Sci. U.S.A. **97**, 5836 (2000).